A&A 446, 583–589 (2006)
DOI: 10.1051/0004-6361:20053032

Astronomy & Astrophysics

The new orbital elements and properties of ε Persei[⋆,⋆⋆]

J. Libich[1,2], P. Harmanec[1,2], J. Vondrák[3], S. Yang[4], P. Hadrava[2], C. Aerts[5,6], P. De Cat[7], P. Koubský[2], P. Škoda[2], M. Šlechta[2], K. Uytterhoeven[2,5], and P. Mathias[8]

[1] Astronomical Institute of the Charles University, V Holešovičkách 2, 180 00 Praha 8, Czech Republic
e-mail: [liba;hec]@sirrah.troja.mff.cuni.cz
[2] Astronomical Institute, Academy of Sciences of the Czech Republic, Fričova 298, 251 65 Ondřejov, Czech Republic
e-mail: [libich;hec;had;koubsky;skoda;slechta;katrienu]@sunstel.asu.cas.cz
[3] Astronomical Institute, Academy of Sciences of the Czech Republic, Boční II/1401a, 141 31 Praha 4, Czech Republic
e-mail: vondrak@ig.cas.cz
[4] Dept. of Physics and Astronomy, University of Victoria, PO Box 3055, Victoria, B.C., V8W 3P6 Canada
e-mail: yang@beluga.phys.uvic.ca
[5] Instituut voor Sterrenkunde, Katholieke Universiteit Leuven, Celestijnenlaan 200 B, 3001 Leuven, Belgium
e-mail: [conny;katrienu]@ster.kuleuven.be
[6] Department of Astrophysics, "Radboud University Nijmegen", PO Box 9010, 6500 GL Nijmegen, The Netherlands
[7] Royal Observatory of Belgium, Ringlaan 3, 1180 Brussel, Belgium
e-mail: peter@ksb-orb.oma.be
[8] Observatoire de la Côte d'Azur Département GEMINI, UMR 6203, 06304 Nice Cedex 4, France
e-mail: mathias@obs-nice.fr

Received 9 March 2005 / Accepted 18 July 2005

ABSTRACT

A detailed analysis of a large collection of electronic spectra from three observatories, together with radial velocities published earlier, were used to derive a new ephemeris and improved orbital elements for the ε Per binary. Observations covering a time interval of about 37 000 days (101.3 years) can be reconciled with a constant orbital period of $14\overset{\mathrm{d}}{.}06916 \pm 0\overset{\mathrm{d}}{.}00004$. The high orbital eccentricity of 0.555 ± 0.009 was also confirmed. New spectral observations confirm that there is a periodic variation of the systemic velocity. Together with new evidence from astrometric observations (also analyzed here), they confirm the existence of a third body in the system with an orbital period of about 9600 days (26.3 years), rather than 4156 days, as reported earlier. Application of the disentangling technique to the Hα spectra with good S/N ratios did not allow detection of spectral lines of either the secondary or tertiary components. For plausible inclinations between 30° and 90°, the observed mass function implies a mass of the secondary $M_2 = 0.85{-}1.77\ M_\odot$, if a primary mass is adopted of $13.5 \pm 2.0\ M_\odot$. Attempts to detect the third body via interferometric observations should continue in spite of this first negative result.

Key words. stars: early-type – stars: binaries: spectroscopic

1. Introduction

Star ε Per (HD 24760, 45 Per, HR 1220, ADS 2888A, HIP 18532; $V = 2\overset{\mathrm{m}}{.}9$) is a well-known bright star, which has been used for a long time as a spectrophotometric and MKK classification standard for the spectral class B0.5 III (Morgan et al. 1943), though it was also classified differently, e.g. B0.5 V (Johnson & Morgan1953). At present it is known as an archetype of early-type line-profile variables and a spectroscopic binary. A detailed history of its investigation is summarized in Tarasov et al. (1995) so need not be repeated here. We mention only their main results and a few subsequent studies relevant to the topic of our paper.

Tarasov et al. (1995) derived the best available orbital elements of ε Per binary (Period: 14.076 days, eccentricity 0.52 etc.) and suggest that the object could even be a triple system, where the third component orbits with a period of 4156 days. De Cat et al. (2000) secured 450 high-dispersion electronic spectra over an interval of 14 consecutive nights, i.e., over one full orbital cycle. They measured radial velocities (RVs) for three Si III lines, using the first normalized velocity moment (Aerts et al. 1992) of the line profiles of the $\lambda\lambda$ 4560 Å Si III triplet. An unconstrained solution of their RVs curve led to an orbital period of $13\overset{\mathrm{d}}{.}8$, but De Cat et al. (2000) then adopted a more accurate period of $14\overset{\mathrm{d}}{.}075$ derived by Tarasov et al. (1995) in their further analyses. Although their systemic

⋆ This research is based on spectra from the Dominion Astrophysical Observatory (DAO), Haute Provence, and Ondřejov.
⋆⋆ Table 1 is only available in electronic form at the CDS via anonymous ftp to cdsarc.u-strasbg.fr (130.79.128.5) or via http://cdsweb.u-strasbg.fr/cgi-bin/qcat?J/A+A/446/583

velocity seems to disagree with the one predicted for the epoch of their spectra based on the 4156-d orbit derived by Tarasov et al. (1995), they point out that they can neither confirm nor rule out the existence of a third body.

Harmanec (1999) analyzed rapid line-profile changes of the long series of Crimean spectra (used in the Tarasov's et al. 1995) and argue that the variations are monoperiodic, with a period of $1^{\rm d}.11878265$ (or its integer multiples) with a very complicated phase curve. Marginal evidence for a similar period was also given by De Cat et al. (2000) in their 14-d series of spectra, but they favour an interpretation in terms of multiperiodic changes, with several short periods having sinusoidal phase curves. Hartkopf et al. (2001) observed ε Per via speckle interferometry and were unable to detect any close visual component.

Since many new electronic spectra have been accumulated in the Ondřejov and Dominion Astrophysical (DAO hereafter) observatories in the meantime, we decided to combine RVs from these spectra both with the data obtained by De Cat et al. (2000) and with all existing RVs to derive an improved ephemeris and reliable orbital elements of the binary. Another goal of this study was to check on the existence of the third body. Finally, the KOREL disentangling technique was used to search for the lines of the secondary component and to remove the orbital RV changes. The residual spectra in the rest frame of the primary will be used for a new analysis of rapid line-profile variations in a follow-up study.

2. Observations and reductions

The new electronic spectra used here consist of the following four data sets:

1. 166 Reticon RF1872 coudé spectrograms from the Ondřejov 2.0-m reflector, with a linear dispersion of 17 Å mm^{-1}, covering the spectral region 6280 to 6720 Å.
2. 19 HEROS CCD échelle spectrograms from the Ondřejov 2.0-m reflector, with a linear dispersion ranging from 3.9 Å mm^{-1} at the blue end to 6.8 Å mm^{-1} near Hα, covering the spectral region 3840 to 8650 Å.
3. 24 CCD700 spectrograms from the Ondřejov 2.0-m reflector coudé slit spectrograph, with a linear dispersion of 17 Å mm^{-1} near Hα, covering the spectral region 6255 to 6767 Å.
4. 230 CCD 4096 spectra, secured by SY at the coudé focus of the 1.2-m reflector of the DAO, with a dispersion of 10 Å mm^{-1}, covering the range 6100–6700 Å.

We also used 450 Haute Provence Observatory (OHP hereafter) spectrograms, which were previously analyzed by De Cat et al. (2000).

Ondřejov's Reticon spectra were completely reduced using the reduction program SPEFO (Horn et al. 1996; Škoda 1996). Initial reductions of the DAO CCD spectra and their conversion into 1D images were carried out by SY, who used IRAF. Initial reductions of the HEROS spectra, including the wavelength calibration, were carried out by MŠ and PŠ within MIDAS using the customized echelle package written by A. Kaufer and O. Stahl. For details see Škoda et al. (2002b). Initial reduction of Ondřejov CCD700 spectra and their optimal extraction into 1D images were carried by PŠ and MŠ in the standard IRAF package "doslit". The wavelength scale was calibrated by fitting Chebychev polynomials up to order 5 to the ThAr arc lines using the IRAF task "identify". For details see Škoda et al. (2002a). All subsequent reductions and the RV measurements were carried out by JL using SPEFO. Wavelength calibration of all Ondřejov Reticon and HEROS spectra and of the majority of DAO CCD spectra was based on ThAr lamps. Several DAO spectra were wavelength-calibrated using CdNe, Ne, and FeAr lamps. For both the Ondřejov and DAO red spectra, the zero point of the wavelength scale was corrected individually through the measurements of selected atmospheric lines; see Horn et al. (1996) for the details. The spectra from those two spectrographs are, therefore, safely on the same heliocentric wavelength scale.

RVs from the DAO and Ondřejov red spectra are solely based on two strong absorption lines: Hα (6562.817 Å) and He I 6678 (6678.151 Å). For consistency, the same lines were also measured in the HEROS spectra for which, however, we also included RVs based on another absorption line; He I 5875 (5875.652 Å). The RV measurements carried out in SPEFO were based on the comparison of a direct and mirror image of the spectral lines in question. Settings were made on the outer wings of the line profiles, less affected by the pronounced line-profile changes.

All RVs with the corresponding heliocentric Julian dates (HJD hereafter) of mid-exposures are listed individually in Table 1 (available only in electronic form). Additionally, we also used all published RVs from photographic and Crimean CCD spectra. The journal of all existing RV data files known to us is given in Table 2. The RV observations by Morrell & Abt (1992) seem to be based on settings on the strong moving sub-features. They do not reflect the true stellar RV. For that reason, we omitted this particular data set from our analyses. For all electronic spectra covering the red region (data files 11, 12, 14, and 15), we obtained an average S/N ratio of 300 in the spectral region near 6700 Å.

Considering the heterogeneity of the data from various sources, we did not adopt the weighting scheme by Tarasov et al. Instead, we first derived a trial solution where all RVs were given equal weight of value 1, and then we made the weight of each dataset inversely proportional to its rms error per one observation derived in the solution. Common weights were used for datasets 1 and 2 or 10 and 11. The weights are in Table 2.

3. New orbital binary solutions

All orbital solutions were derived with the Fortran program FOTEL (version 4), developed by Hadrava (1990, 2004a). We used weights (as explained in the previous section) and all reliable data, but we did not include the source 9, which was very strongly influenced by rapid line changes and the first measurement of the source 1 (with an unrealistic value -51 km s^{-1}). We first investigated the secular constancy of the orbital period and a possible apsidal advance, and no changes were detected.

Table 2. Journal of RV observations.

Source	Epoch (JD−2 400 000)	No. of obs.	Disp. (Å mm^{-1})	Weight	Spectral region
1	16421–16806	2	10.9	0.30	4500 Å
2	16426–17856	9	30	0.30	4500 Å
3	17895–19409	66	40	0.57	
	17895–17916	5	40		3900–4900 Å
	18634–18721	16	40		3900–4900 Å
	18955–19117	32	40		3900–4900 Å
	19335–19409	13	40		3900–4900 Å
4	22276–22277	2	33.4	0.52	Hα
5	45669–47885	29	15–30	0.58	
	45669–45670	20	15		4500–4950 Å
	47813–47814	3	15		4060–4500 Å
	47885	6	30		5800–6700 Å
6	46334–46761	7	4.6–9.1	2.37	
	46334	2	9.1		6500–6720 Å
	46405	1	4.6		triplet Si III
	46757–46761	4	4.6		triplet Si III
7	47104–48690	27	4.2–8.5	1.27	
	47104–47115	10	8.5		3500–5000 Å
	47104	2	6.3		6200–6700 Å
	48600–48690	13	4.2		4000–4900 Å
	48607	1	4.2		3500–4400 Å
	48679	1	8.5		3500–5000 Å
8	47375–49205	555/69	3–6	0.77	
	47375–47410	7	3		Hα
	47382–47407	117/14	3		He I 6678
	47410	17	6		Hα
	47553–47569	3/0	3		He I 6678
	47569–47570	22/8	3		He I 5875
	47721–47767	287/33	3		He I 6678
	48143–48245	98/11	3		He I 6678
	48646	3/3	3		He I 6678
	49205	1	6		Hα
9	47511–48271	27	15		Hγ, He I 4471, Mg II 4481
10	47828	2	17.2	1.74	4250–4750 Å
11	49019–51524	166	17.2	1.74	6300–6700 Å
12	49574–53276	230	10	1.75	6200–6800 Å
13	50373–50386	450	1.7	3.30	triplet Si III
14	52510–52698	19	6.8	1.52	5850–8350 Å
15	52877–53409	26	17.2	1.43	6255–6767 Å
Summary	16421–53409	1617	1.7–40	0.30–3.30	3500–8350 Å

Details on sources of data and instruments used:

1 ... Campbell & Moore (1928): Lick 0.91-m refractor, New Mill's spg., photographic plates.

2 ... Frost et al. (1926): Yerkes 0.40-m refractor, 1-prism Bruce spg., photographic plates.

3 ... Beardsley (1969): Allegheny 0.79-m Keeler Memorial reflector, 1-prism Mellon spg., photographic plates.

4 ... Henroteau (1922): Ottawa 0.38-m refractor, 2-prism spg., photographic plates.

5 ... Tarasov et al. (1995): DAO 1.83-m reflector, Cassegrain grating spg., Reticon RL 1872F/30.

6 ... Gies & Kullavanijaya (1988) + Gies (priv. com., HJD 46334): McDonald 2.7-m reflector, coudé grating spg., Octicon detector (8xRL 1872F/30 Reticon).

7 ... Tarasov et al. (1995): Ondřejov 2.0-m reflector, coudé grating spg., blue photographic plates.

8 ... Tarasov et al. (1995): Crimean Astrophysical Observatory 2.6-m reflector, coudé grating spg. with a 576 × 380-pixel GEC CCD, (in column No. of obs. RVs from all profiles/RVs from only symmetric He I 6678 profiles).

9 ... Morrell & Abt (1992): Kitt Peak 1.0-m reflector, coudé grating spg., blue Texas Instruments CCD 800 × 800 pixels spectrograms.

10 ... Tarasov et al. 1995): University of British Columbia 0.4-m reflector, blue Reticon RL 1872F/30 spectra.

11 ... This paper: Ondřejov 2.0-m reflector, coudé grating spg., Reticon RL 1872F/30 (with 15 μm pixels) red spectra.

12 ... This paper: DAO 1.2-m reflector, coudé grating spg. with a thick Loral 4096 × 200 CCD device (15 μm pixels), red spectra.

13 ... De Cat et al. (2000) and this paper: Observatoire de Haute Provence (OHP) 1.52-m reflector, AURELIE spg., CCD EEV (2048 × 1024 pixels) spectra centred to 4560 Å.

14 ... This paper: Ondřejov 2.0-m reflector, HEROS échelle spg.

15 ... This paper: Ondřejov 2.0-m reflector, CCD700 slit spg.

For the Allegheny RVs, we applied the correction quoted by Beardsley (1969) to get them on the standard GCVS system of velocities. This was not possible for other data sets. We adopted the joint zero point for new data sources 11, 12, 14, and 15, which were corrected via telluric lines as explained above. Libich et al. (2003) used these data to test the reality of the variations in the γ velocity.

To this end, we derived the binary solution for the joint zero points of all RVs for the combination of all sources as solution 1 (unweighted) or solution 2 (weighted) and for individual systemic RVs for individual data sets sorted by the time as solution 3 (unweighted) or solution 4 (weighted). Each data set has the time range mostly shorter than 200 days, with only 2 cases between 300–400 days, which is adequate for the possibility of the modeling of the γ velocity variations. We were limited to only 30 datasets of the program FOTEL4.

Since our trial secular solutions showed that the γ velocity changes with epoch, it was not possible to solve for systematic errors among the older velocity sets. The secular γ velocities for each dataset are summarized in Table 4.

We adopted solution 4 as final binary solution with secular changes of systemic velocity, because it is more realistic and it comprises the changes of the systemic (γ) velocity. We found that all RVs can be reconciled with a single period of $14\overset{\mathrm{d}}{.}06915$. This is also documented by phase plots of separate data subsets for this period and solution 4 shown in Fig. 1.

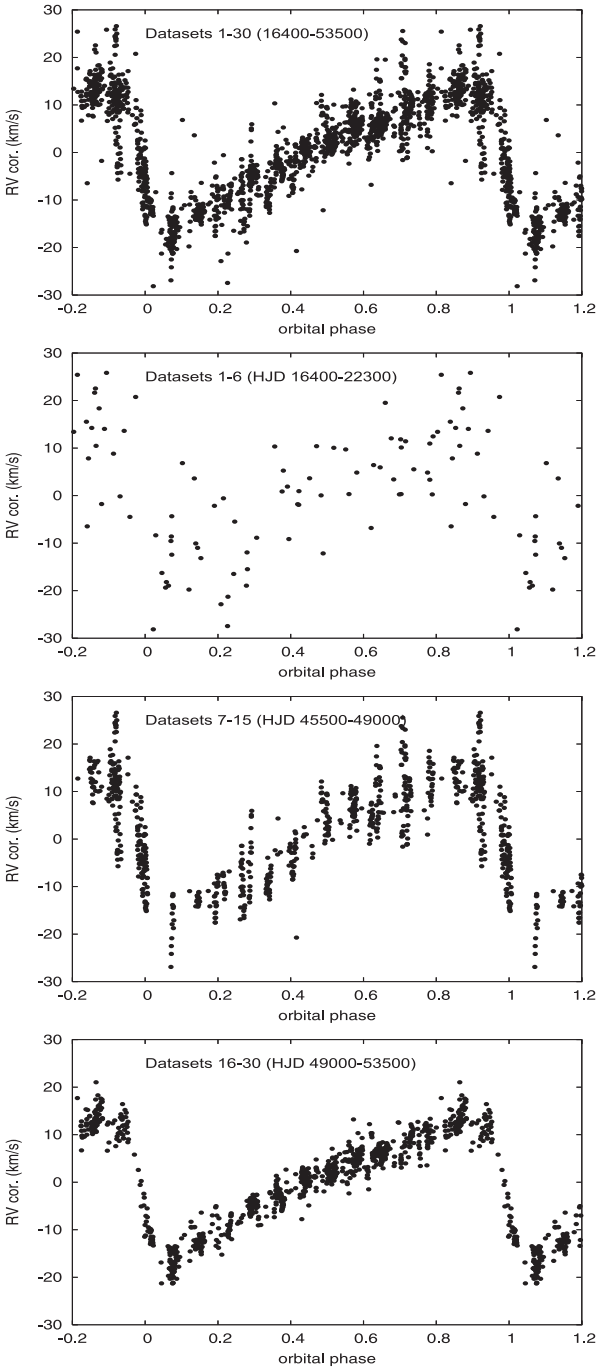

Fig. 1. *From top to bottom*: the RV curves (corrected by γ velocity) phased according to orbital period $14\overset{\mathrm{d}}{.}06915$ and the elements from solution 4 for all data and for the datasets sorted by time from the oldest datasets to the newest datasets (see Table 4).

4. New orbital solutions of the third body

Tarasov et al. (1995) suggested a triple star orbital solution for the system of ε Per with a period of 4156 days (11.38 years). Figure 2 shows that their suggestion of a significant slow variation of the γ velocity is confirmed by our larger data set. We have included all of the data available to us in Fig. 2, even though some data sets have insufficient phase coverage of the short period binary orbit to accurately determine the γ velocity for that epoch.

To verify the existence of a third body, which would manifest itself as a slow variation of the systemic γ velocity, we derived its period. It is obvious, however, that the period of 4156 days (11.38 years) is no longer tenable, because Tarasov et al. had data from only two ascending parts of the RV curve for the long period orbit and there was no coverage for the maximum of RV curve. Without any more sophisticated period analysis, one can also see that the orbital period of the third body must be longer than some 7000 days. Two similar steep increases in the γ velocity seen in the early and more recent data (see the upper panel of Fig. 2) are separated by 78 years. This also defines the upper limit for the largest possible orbital period of the third body. The only other possible periods could be approximate integer submultiples (n) of this value, namely 39.0 years (2), 26.0 years (3), or 19.5 years (4), and for shorter periods than 7000 days: 15.6 years (5), 13.0 years (6), 11.1 years (7) (near the period derived by Tarasov et al. 1995), and 9.8 years (8). The main uncertainty stems from the facts that the available data do not cover the phases of γ velocity minima and that there are only the parts of two cycles; therefore, with different values of eccentricity, one can reconcile the available data with any of the above possible periods. Continuing observations and/or inspection of data archives and measuring RVs for the time interval between JD 2 420 000 and 2 445 000 would be very desirable.

We detected the most probable period 9428 days (25.8 years) from PDM (phase dispersion minimization) period analysis (according to Stellingwerf 1978), but there is a range of periods between 9400 days (25.7 years) and 9600 days

Table 3. FOTEL orbital solutions for the 14-d binary orbit for all RV data (only all measurements of source 9 and one measurement of source 1 were not included). All epochs are in HJD-2 400 000. Column "rms" gives the mean rms error of one observation of unit weight for each solution; all errors quoted with individual elements are rms errors of these elements calculated from the covariance matrix.

Element	Solution 1	Solution 2	Solution 3	Solution 4
Data sources	All but 9+1/1	All but 9+1/1	All but 9+1/1	All but 9+1/1
No. of RVs	1588	1588	1588	1588
Weighting	unweighted	weighted	unweighted	weighted
P (d)	14.069352	14.069069	14.069151	14.069145
	± 0.000053	± 0.000047	± 0.000094	± 0.000083
$T_{\rm periastr.}$	47767.563	47767.565	47767.500	47767.531
	± 0.054	± 0.035	± 0.033	± 0.022
$T_{\rm RVmax}$	47765.426	47765.667	47765.778	47765.915
$T_{\rm RVmin}$	47768.627	47768.499	47768.499	47768.415
e	0.464 ± 0.014	0.510 ± 0.011	0.516 ± 0.011	0.5470 ± 0.0070
ω (°)	109.3 ± 2.1	108.9 ± 1.5	104.4 ± 1.5	105.62 ± 0.89
K_1 (km s^{-1})	14.21 ± 0.29	14.48 ± 0.23	14.99 ± 0.23	15.24 ± 0.14
γ (km s^{-1})	8.87 ± 0.14	9.90 ± 0.11	variable	variable
rms (km s^{-1})	5.50	3.74	4.13	2.97
$f(m)$ ($M_\odot$)	0.002909	0.002818	0.003089	0.003026

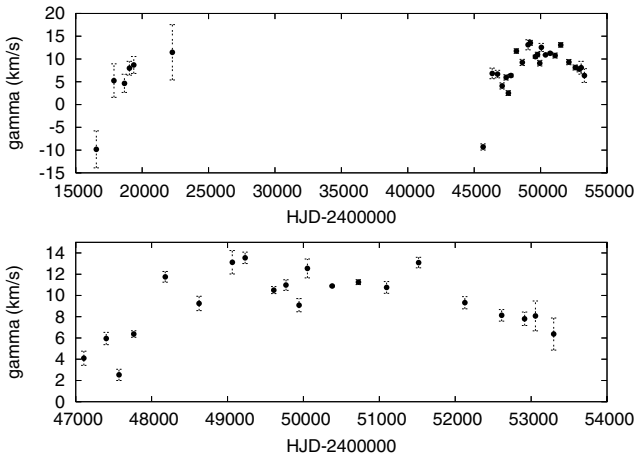

Fig. 2. A plot of locally derived γ velocities vs. time (Table 4): *top*: all available data; *Bottom*: the last orbital cycle only.

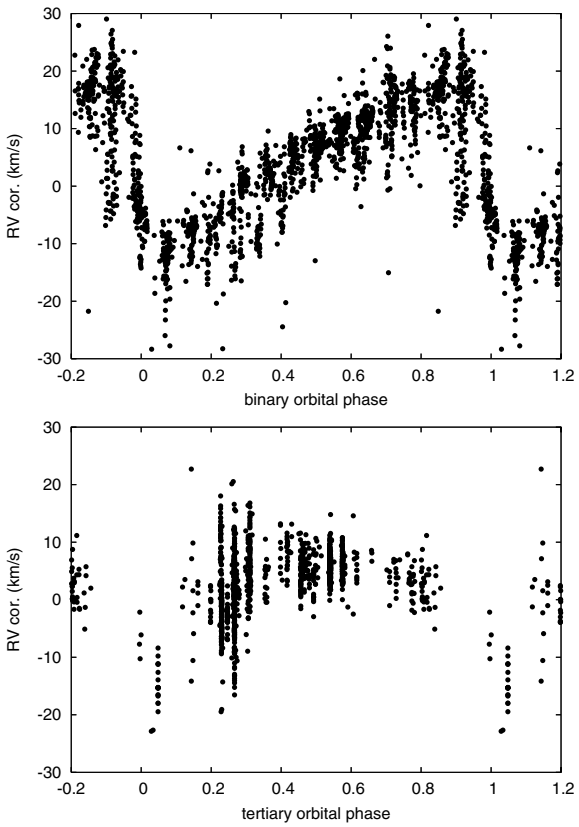

Fig. 3. *From top to bottom*: the binary RV curve (corrected by γ velocity) phased according to binary orbital period 14$^{\rm d}$.06916 and the elements from solution 6 and tertiary RV curve phased according to tertiary orbital period 9577 days (see Table 5).

(26.3 years), which correspond approximately to the submultiple $n = 3$.

We also derived the trial triple–star orbital solution (see Table 5) for the same data and obtained new orbital periods and elements of the binary and tertiary orbit: 14$^{\rm d}$.06916 and 9577 days (26.22 years). The phase plots for both periods are found in Fig. 3. The estimates of the mass of the secondary and the tertiary component and the mass ratios were derived from the mass functions of triple-star orbital solution 6 (see Table 6).

Adopting electronic spectra from sources 11–15, we attempted to also analyse them by the method of spectral disentangling (Hadrava 1995, 2004b). We used a new version of the program KOREL in the region around the Hα profile where a secondary of any spectral class should in principle be detectable. Only spectra with a signal-to-noise ratio $S/N \geq 300$, corrected to the common zero point via measurements of telluric lines, were used. The spectra were given weights proportional to the square of the measured S/N ratio. To see the consistency of the results, we analyzed 292 spectra altogether, which were divided into 5 time intervals (HJD 2 449 000–2 449 500, 2 449 500–2 450 000, 2 450 000–2 450 500, 2 450 500–2 451 000, and later than 2 452 000). KOREL led to a very similar solution to solution 2 (see Table 3) for the primary. Also the telluric spectrum was disentangled

Table 4. Local values of the γ velocity assuming solution 4.

No.	Mean epoch (HJD-2 400 000)	Mean epoch (year)	No of sp.	γ (km s^{-1})
1	16550.8	1904.192	7	-9.8 ± 4.1
2	17880.7	1907.833	8	5.3 ± 3.7
3	18664.8	1909.979	16	4.7 ± 2.0
4	19043.4	1911.016	32	8.0 ± 1.5
5	19371.7	1911.916	13	8.7 ± 1.9
6	22277.3	1919.871	2	11.5 ± 6.1
7	45669.9	1983.916	20	-9.31 ± 0.67
8	46358.6	1985.800	3	6.8 ± 1.2
9	46760.0	1986.900	4	6.68 ± 0.82
10	47107.4	1987.852	12	4.09 ± 0.67
11	47401.9	1988.657	141	5.95 ± 0.58
12	47569.1	1989.114	25	2.53 ± 0.53
13	47764.2	1989.648	298	6.37 ± 0.31
14	48179.0	1990.785	98	11.75 ± 0.50
15	48625.6	1992.009	18	9.25 ± 0.67
16	49061.9	1993.201	10	13.1 ± 1.1
17	49231.2	1993.665	22	13.54 ± 0.54
18	49609.5	1994.701	78	10.51 ± 0.33
19	49770.4	1995.142	22	10.98 ± 0.50
20	49941.7	1995.612	26	9.09 ± 0.62
21	50052.6	1995.915	6	12.54 ± 0.89
22	50378.6	1996.806	546	10.888 ± 0.070
23	50723.8	1997.752	95	11.25 ± 0.23
24	51095.8	1998.771	11	10.76 ± 0.55
25	51517.3	1999.926	3	13.10 ± 0.50
26	52127.1	2001.593	16	9.32 ± 0.58
27	52612.3	2002.923	24	8.13 ± 0.55
28	52914.5	2003.751	18	7.80 ± 0.63
29	53056.8	2004.140	8	8.1 ± 1.4
30	53297.8	2004.799	7	6.4 ± 1.5

Table 5. FOTEL orbital solution for the triple star and binary orbit for all RV data (only all measurements of source 9 and one measurement of source 1 were not included). All epochs are in HJD-2 400 000. Column "rms" gives the mean rms error of one observation of unit weight for each solution; all errors quoted with individual elements are rms errors of these elements calculated from the covariance matrix.

Element	Solution 5	Solution 6
Data sources	All but 9+1/1	All but 9+1/1
No. of RVs	1588	1588
Weighting	unweighted	weighted
P (d)	14.069140	14.069161
	$\pm$ 0.000047	$\pm$ 0.000038
$T_{\rm periastr.}$	47767.522	47767.543
	$\pm$ 0.032	$\pm$ 0.024
$T_{\rm RVmax}$	47765.859	47765.956
$T_{\rm RVmin}$	47768.478	47768.400
e	0.530 ± 0.011	0.5549 ± 0.0093
ω (°)	104.6 ± 1.5	105.8 ± 1.2
K_1 (km s^{-1})	15.05 ± 0.22	15.23 ± 0.20
$f(m)$ ($M_\odot$)	0.003036	0.002964
P' (d)	9611.	9577.
	$\pm$ 44.	$\pm$ 35.
P' (years)	26.31	26.220
	$\pm$ 0.12	$\pm$ 0.094
$T'_{\rm periastr.}$	35797.	35632.
	$\pm$ 169.	$\pm$ 116.
$T'_{\rm RVmax}$	31288.	31465.
$T'_{\rm RVmin}$	35841.	35712.
e'	0.443 ± 0.029	0.474 ± 0.027
ω' (°)	175.2 ± 5.1	170.4 ± 3.3
K_{1+2} (km s^{-1})	10.42 ± 0.56	10.84 ± 0.62
$f'(m)$ ($M_\odot$)	0.8127	0.8287
$\gamma_{\rm joint}$ (km s^{-1})	5.27 ± 0.28	5.23 ± 0.23
rms (km s^{-1})	4.34	3.13

without problems, but no convincing evidence of the Hα line from the secondary was found for any of the data subsets or for the complete set of 292 spectra. We did not detect the lines of the possible third body (tertiary) in the system from solution 6 (see Table 5). We, therefore, postpone this problem to the future.

At this moment, we only present improved estimates of the properties of the binary and the tertiary based on the mass function resulting from solution 6: 0.002971 $M_\odot$. For various possible inclinations of the binary (resp. tertiary long period) orbit from 90° to 30°, and the adopted mass of the primary component ((13.5 ± 2.0) $M_\odot$), the mass ratio of the secondary ranges from 0.06 to 0.13 (similar to the values from 0.07 to 0.148 derived by Tarasov et al. 1995) and of the tertiary from 0.51 to 1.39 (very different from the values from 0.16 to 0.354 in Tarasov et al. 1995). Specific values for several inclinations can be found in Table 6. The values of the tertiary mass are very uncertain, because we do not know the minimum for the RV curve of the tertiary and were not able to derive an unambigously reliable value of the amplitude for the RV curve of the long period orbit K_{1+2}. From the spectrum analysis (the tertiary was not detected) and the estimates of the tertiary mass (Table 6), it seems that the inclination of the long period orbit is lower than 45 degrees.

5. Astrometric analysis

We used astrometric observations from several observatories homogenized by J. Vondrák (JV). We averaged all data during each year and recalculated them to the same system of measured deviations of calculated instantaneous absolute coordinates (dα and dδ). This system is connected to a measured (observed) right ascension and declination of a photocenter which is probably identical with the primary component. Basic information on all data sources is given in Table 7. We also included 4 yearly mean positions from the HIPPARCOS satellite by ESA(1997).

All data were reduced by two authors, Jan Libich (JL) and Jan Vondrák (JV), independently. We used the program BINARY (Gudehus 2001, 2004) for a calculation of orbital parameters for an orbit of the third body. It allows 2-D astrometric positional ($XY-\alpha$ and δ) to be combined with spectroscopic data, in order to simultaneously solve for the orbital elements and other parameters.

We only derive a trial solution for the other elements based on solution 6. Unfortunately we did not have sufficiently accurate astrometry to derive a complete free solution. We were also not sure that the photocenter of ε Per , observed by optical astrometry, and the photocentric position of its primary were

Table 6. Estimates of the mass ratio $q = M_2/M_1$ and $q' = M_3/(M_1 + M_2)$, the mass of the secondary M_2 and of the tertiary M_3 for various possible orbital inclinations i of the binary and i' of the tertiary orbit. They are based on the primary mass derived by Tarasov et al. (1995) $M_1 = 13.5 \pm 2.0\ M_\odot$ and on the mass function from solution 6.

$\sin i$	i	q	$M_2\ (M_\odot)$
1.0	90°	0.131 ± 0.012	1.77 ± 0.17
0.9	64°	0.107 ± 0.010	1.45 ± 0.14
0.8	53°	0.091 ± 0.009	1.23 ± 0.12
0.7	44°	0.079 ± 0.007	1.07 ± 0.10
0.6	37°	0.070 ± 0.007	0.95 ± 0.10
0.5	30°	0.063 ± 0.006	0.85 ± 0.09
$\sin i'$	i'	q'	$M_3\ (M_\odot)$
1.0	90°	1.39 ± 0.12	18.7 ± 1.6
0.9	64°	1.040 ± 0.099	14.0 ± 1.3
0.8	53°	0.828 ± 0.083	11.2 ± 1.1
0.7	44°	0.687 ± 0.071	9.27 ± 0.96
0.6	37°	0.586 ± 0.063	7.91 ± 0.85
0.5	30°	0.510 ± 0.056	6.89 ± 0.76

Table 7. Journal of ground-based astrometric measurements.

Observatory position	No. of obs.	Instrument of obs.	Years of obs.
Wuhan	752	AL	1964–86
Pecný	13	CZ	1970–91
Praha 2	25	CZ	1980–84
Praha 6	39	CZ	1985–91
Bratislava	30	CZ	1987–91
Charkov	59	PTI	1973–91
Nikolaev	22	PTI	1975–91

Remarks: AL ... astrolabe, CZ ... circumzenithal.
PTI ... photoelectric transit instrument.

identical. We attempted to calculate all other basic parameters for this fixed parameter of solution 6 using the combination of astrometric and spectroscopic data and a fixed HIPPARCOS parallax $\pi = 0\farcs00606 \pm 0\farcs00082$.

The BINARY solution of the orbital elements from the combination of the spectroscopic and astrometric data does not conflict with the FOTEL solution, but it was impossible to improve orbital elements. We conclude that no reliable estimate of the tertiary mass is possible at present, because we did not know enough accurate values for the amplitude of RV K_{1+2}, joint systemic velocity $\gamma_{\rm joint}$, and the inclination i of the tertiary orbit. Hence, we decided to omit all analyses, solutions, tables, and figures.

6. Conclusion

An analysis of a large collection of spectra of ε Per has led to determination of substantially improved ephemeris and orbital elements. However, attempts to disentangle the lines of either the secondary or tertiary were unsuccessful, probably because they are both too faint in comparison to the primary, or the orbital elements of the tertiary are not too accurate for the KOREL disentangling.

Adopting the properties of the primary after Tarasov et al. (1995) and the range of plausible mass ratios derived here, we estimate the mass of the secondary to be $M_2 = 0.85{-}1.77\ M_\odot$. If the secondary is a main-sequence star, its probable radius is $R_2 = (1.4 \pm 0.4)\ R_\odot$, which implies a spectral class somewhere between A6 V and K1 V. The mass of the tertiary must be larger.

The existence of the third body with an orbital period of about 26 years now seems to be safely confirmed, from the slow change of the γ velocity of the $14\fd0$ binary, triple-star solution in FOTEL and it also seems not to conflict with the available astrometric observations, though this later piece of evidence is currently rather uncertain because of the limited accuracy of the astrometry.

Acknowledgements. The use of the computerized bibliography from the Strasbourg Astronomical Data Centre is gratefully acknowledged. This study was realized as a part of the research projects J13/98: 113200004, AV 0Z1 003909, and K2043105.
One of the authors, J.V., acknowledges the support provided by the grant No. IAA3003205 awarded by the Grant Agency of the Academy of Sciences of the Czech Republic.

References

Aerts, C., de Pauw, M., & Waelkens, C. 1992, A&A, 266, 294
Beardsley, W. R. 1969, Public Allegheny Observatory, Univ. Pittsburg, 8, 7
Campbell, W. W., & Moore, J. H. 1928, Publ. Lick Obs., 16, 1
De Cat, P., Telting, J., Aerts, C., & Mathias, P. 2000, A&A, 359, 539
ESA 1997, The Hipparcos and Tycho Catalogues, ESA SP-1200
Frost, E. B., Barett, S. B., & Struve, O. 1926, ApJ, 64, 1
Gies, D. R., & Kullavanijaya, A. 1988, ApJ, 326, 813
Gudehus, D. H. 2001, BAAS, 197, 470
Gudehus, D.H. 2004, User guide: `http://www.chara.gsu.edu/~gudehus/binary.html`
Hadrava, P. 1990, Contr. Astron. Obs. Skalnaté Pleso, 20, 23
Hadrava, P. 1995, A&AS, 114, 393
Hadrava, P. 2004a, Publ. Astron. Inst. ASCR, 92, 1
Hadrava, P. 2004b, Publ. Astron. Inst. ASCR, 92, 15
Harmanec, P. 1999, A&A, 341, 867
Hartkopf, W. I., McAlister, H. A., & Mason, B. D. 2001, AJ, 122, 3480
Henroteau, F. 1922, Publ. Dom. Astrophys. Obs., 5, 331
Horn, J., Kubát, J., Harmanec, P., et al. 1996, A&A, 309, 521
Johnson, H. L., & Morgan, W. W. 1953, ApJ, 117, 313
Libich, J., Harmanec, P., Yang, S., et al. 2003, Proc. of the 12th Annual Conference of Doctoral Students – WDS 2003, Part III: Physics, 496
Morgan, W. W., Keenan, P. C., & Kellman, E. 1943, Chicago, Ill. (The University of Chicago press)
Morrell, N., & Abt, H. A. 1992, ApJ, 393, 666
Škoda, P. 1996, ADASS V, ASP Conf. Ser., 101, 197
Škoda, P., Šlechta, M., & Honsa, J. 2002a, Publ. Astron. Inst. ASCR, 90, 22
Škoda, P., Šlechta, M., & Honsa, J. 2002b, Publ. Astron. Inst. ASCR, 90, 40
Stellingwerf, R. F. 1978, ApJ, 224, 953
Tarasov, A. E., Harmanec, P., Horn, J., et al. 1995, A&AS, 110, 59